A strong robust DC-DC converter of all-digital high-order sliding mode control for fuel cell power applications

Yu Wu, Yigeng Huangfu, Rui Ma, Alexandre Ravey, Daniela Chrenko

A strong robust DC-DC converter of all-digital high-order sliding mode control for fuel cell power applications

Yu Wu[a,b,**], Yigeng Huangfu[c,*], Rui Ma[c], Alexandre Ravey[a,b], Daniela Chrenko[a,b]

[a] FEMTO-ST Institute, CNRS, Univ. Bourgogne Franche-Comte, UTBM, Belfort, France
[b] FCLAB, CNRS, Univ. Bourgogne Franche-Comte, UTBM, France
[c] School of Automation, Northwestern Polytechnical University, PR China

In the fuel cell power applications, the output voltage and load power are variable which highly depends on the operating conditions. Thus, DC/DC power converters are usually utilized to obtain a constant voltage to match the subsequent power bus. Due to the non-linear characteristics of the fuel cell and load profiles, a stronger robustness design of power converters is required. In order to resolve the above issues, this paper designs a strong robust isolated flyback DC/DC converter for the fuel cell power applications. An all-digital controller based on high-order sliding mode (HSM) control is developed. The super-twisting algorithm of HSM is applied with a digital signal processor (DSP) TMS320F28035 that is used as the control chip. In the experiments, the designed digital HSM controller can achieve a fast convergence with a settling time of less than 0.1 ms and an overshoot of less than 0.1%. A typical incremental PI controller is also designed as the benchmark control method. The effectiveness of the proposed digital HSM controller is demonstrated through several different experiments conducted under large disturbances of load and input voltage.

1. Introduction

Fossil energy has been regarded as increasingly deficient in recent decades and it has become increasingly crucial to seek alternative, sustainable energy sources. Renewable energy sources have received great attention, including wind turbine generation, solar generation, and hydrogen fuel cells. Such applications of renewable energy can resolve the energy crisis to a certain extent and mitigate the environmental issues caused by fossil fuels. However, the renewable energy generation (REG) is generally unpredictable, intermittent, and variable, which significantly affects the system stability [1]. For the fuel cell power applications, the output voltage highly depends on its output

* Corresponding author. School of Automation, Northwestern Polytechnical University, PR China.
** Corresponding author. FEMTO-ST Institute, CNRS, Univ. Bourgogne Franche-Comte, UTBM, Belfort, France.
E-mail addresses: yu.wu@utbm.fr (Y. Wu), yigeng@nwpu.edu.cn (Y. Huangfu).

current due to its non-linear volt-ampere characteristics [2,3]. Meanwhile, the generation power of fuel cells is also affected by the operating conditions, such as the inlet pressure, the stack temperature, and the flow rates of hydrogen and air, etc. [4]. Thus, a DC/DC power converter is generally used to regulate the fuel cell generation power in order to obtain a constant output voltage to match the subsequent electrical power bus.

The controller design of power converters is generally based on the small signal control theory proposed by Middlebrook and Cuk in Ref. [5]. Due to its simplicity and practicality, the feedback control of power converters based on the small signal model is widely applied at present. However, in order to linearize the nonlinear characteristics of power converters, the small signal control model assumes that the system operates at a single steady state point, which can only ensure the small signal stability around the steady point. Thus, when the system encounters a large disturbance input, the system output will become unstable [6].

The classical linear control algorithms include the PI control, and PID control, etc., which are suitable to be applied in a linear time-invariant system. However, the power converter is a typical non-linear non-singular system with variable input, and the system often operates at different steady states with variable load and input. Hence, a robust voltage controller is necessary considering the non-linear characteristics of the fuel cell, the power converter, as well as the load. Increasing studies about the robust control for the fuel cell power applications have been conducted with the aim of resolving this issue [7–10].

In order to resolve the deficiency of the linear control, many non-linear control theories have been developed, such as fuzzy control [11,12], neural network-based control [13,14], adaptive control [15,16], and sliding mode control [17]. As one of the non-linear control methods, sliding mode control (SMC) is notable for its simple structure and insensitivity to both its internal parameter and any external disturbance [18]. However, the conventional sliding mode control (CSMC) is marked by the chattering issue due to its discrete control law, which might lead to high-frequency vibration of the system [19]. In order to resolve this issue, the high-order sliding mode (HSM) control is developed [20,21]. The high-order sliding mode (HSM) is a generalization of the conventional sliding mode control, which means the chattering issue is eliminated while the advantages of CSMC are retained. Due to the superior characteristics of the developed sliding mode control systems, researchers have shown an increased interest in its power converter applications [22–34].

In Ref. [22], Martinez-Salamero et al. introduced a sliding mode controller to minimize the inrush current and to provide output voltage regulation for the boost converters. In Ref. [23], Lopez-Santos et al. presented a robust sliding mode controller for a quadratic boost converter. Here, the inner loop was based on an analog sliding mode controller, while the outer loop was based on a proportional-integral compensator. Meanwhile, in Ref. [24], Chincholkar et al. proposed an improved pulse-width-modulation (PWM)-based sliding mode controller for a 2-stage dc/dc cascade boost converter, which expanded the application range of SMC. In addition, in order to simplify the controller design, some digital sliding mode controllers are also developed. In Ref. [25], a digital CSMC was designed to adjust the duty cycle for a buck converter that operates on a fixed switching frequency. However, while the fixed switching approach includes the advantage of the digital pulse-width-modulation technique, it slows down the dynamic response significantly [28]. In Refs. [26,27], a digital SMC was implemented in the frequency domain by reformulating the sliding mode control. However, the dynamic response shows large transient excitation in this kind of approach. Furthermore, the sliding mode control is also developed to realize the maximum power point tracking (MPPT) function in the boost-PV system [29,30]. Nevertheless, the studies in Refs. [22–30] based on the conventional sliding mode control (CSMC) suffer from a relatively long convergence time [21,34], while the attendant chattering issue remains another concern. In order to decrease the convergence time and improve the stability, several advanced sliding mode control strategies are investigated in Refs. [31–34]. In Ref. [31], a second-order sliding mode control algorithm was developed for a boost DC/DC converter to maximize the power generated from the fuel cell. Similarly, a double integral sliding mode controller for a PV-boost energy harvesting system was proposed in Ref. [32]. Another second-order sliding mode control based on twisting algorithm was implemented in a buck DC/DC converter to improve the robustness [33]. In Ref. [34], a switching sliding mode control strategy was developed for a buck converter. A specialized analog control circuit composed of exponential operators and multipliers was designed to realize the switching sliding mode control. However, the techniques suggested in Refs. [31–34] require the specialized design of the analog controller circuit. Thus, due to the complexity of the analog controller design, their application in the engineering projects is further limited.

In this paper, an all-digital HSM controller based on the super-twisting algorithm is designed for the flyback DC/DC converter. The flyback converter is a classical isolated DC/DC converter that has both buck and boost capability. It is widely used in various types of industrial power applications due to its simple structure, low manufacture cost, and isolated conversion. Besides, it is not an issue to have more than one output on a single transformer while the output voltage can be either negative or positive. The flyback converter is also preferred in terms of fuel cell applications to harvest the generated energy [35,36]. However, the flyback converters have a zero point in the right-half plane of their transfer function. This zero point seriously affects the dynamic performance and cannot be eliminated through feedback control [37]. Therefore, it is valuable to improve the robust performance of this type of power converter.

The work in this study is also compared with other reported studies (see Table 1) in terms of application scenarios, control algorithms, implementation techniques, and verification methods.

From the summary of these studies presented in Table 1, it is clear that the robust controller design of isolated flyback DC/DC converters has not been sufficiently studied as of yet. In fact, though some studies

Table 1
Comparisons of this work and other related studies.

Literature	Power Converter	Control Strategy	Implementation	Verification
2013, L. Martinez-Salamero et al. [22]	Boost	CSMC	Analog	Experiment
2015, A.Dashtestani et al. [28]	Buck	CSMC	Digital	Experiment
2015, O. Lopez-Santos et al. [23],	Boost	CSMC	Analog	Simulation
2017, M. Farhat et al. [29]	Boost	CSMC	N/A	Simulation
2017, S.H.Chincholkar et al. [24]	Cascade Boost	CSMC	Analog	Experiment
2017, M. Derbeli et al. [31]	Boost	HSM (Super twisting)	Analog	Simulation
2017, N. Chatrenour et al. [32]	Boost	Integral SMC	N/A	Simulation
2017, S. M. Rakhtala et al. [33]	Buck	HSM (Twisting)	Analog	Experiment
2018, B. Wang et al. [34]	Buck	Switching SMC	Analog	Experiment
This work	Flyback	HSM (Super twisting)	Digital	Experiment

on HSM control have emerged for boost and buck converter applications, the reported experimental studies are still lacking. It is noted that the experimental studies are highly valued in the power electronic area, which appears to be more instructive and convincing for practical engineering. Furthermore, the earlier works largely focus on applying the sliding mode control in different applications while they tend to neglect the difficulty of implementing the nonlinear controller within engineering projects. Compared to the analog SMC present in these studies, the digital sliding mode controller is of great advantage which is more practical and more economical in the industrial applications [28,38]. On the basis of the above considerations, the proposed all-digital HSM controller is an attempt to provide a solution for the robust control of the flyback DC/DC converter, and detailed experiments are conducted accordingly. The major contributions of this work thus include the following:

1) An all-digital high-order sliding mode controller is designed for the flyback DC/DC converter.
2) The HSM control based on the super twisting algorithm is formulated into a digital hysteretic control manner to be applied in a flyback converter with a common digital signal processor TMS320F28035.
3) Detailed experiments under both input voltage disturbance and load disturbance are conducted to verify the effectiveness of the proposed digital HSM control method.
4) A typical incremental PI controller is designed as the benchmark control algorithm in the experiments. Detailed comparisons between the HSM control and the PI control are conducted.

The structure of this paper is organized as follows. Section II gives a brief overview of the fuel cell power system and presents the non-ideal model of the flyback DC-DC converter. Section III then introduces the proposed all-digital HSM controller in details, while an incremental PI controller is designed as the benchmark. Meanwhile, in Section IV, the experiments under different disturbance conditions are presented, and the performance comparisons between the digital HSM controller and the incremental PI controller are conducted and analyzed. Finally, our conclusions are drawn in Section V.

2. System modelling

2.1. Overview of fuel cell power system

The proposed fuel cell power system model is shown in Fig. 1 (a), similar to our previous work in Ref. [39]. The fuel cell is fed by heated hydrogen, and the water vapor is added in order to keep the humidity of the membrane between the electrodes. Then, the fuel cell can convert the energy stored in the fuel directly into the electricity as the power input of the flyback DC/DC converter. In order to test the dynamic performance of the converter, a controllable variable load is added. The converter output voltage will be sampled for the control of the switches. After the sliding mode control module receives the feedback voltage signal, an updated digital signal will be delivered to the converter for the robust control.

2.2. Non-ideal flyback converter model

The topology of flyback DC-DC converter is shown in Fig. 1(b). E_{cell} is the DC power supply, T is the transformer, S is the switch, C is the output capacitor, R is the resistive load, V_c is the output voltage. The static voltage gain $M(D)$ of flyback converter operating in continuous conduction mode without considering the power losses can be described in (1) as follows:

$$M(D) = \frac{V_c}{E_{cell}} = \frac{n \cdot D}{1 - D} \tag{1}$$

where D is the duty cycle, n is the transformer turns ratio. From the voltage gain in formula (1), we can know that the flyback converter can either step-up or step-down the input voltage, which provides a flexibility for the subsequent power bus voltage. Moreover, the transformer of the flyback converter provides another degree of freedom for the voltage gain, as well as the capability of isolating different power sources.

When the switch is on, the inductor current of primary side transformer starts to increase, the diode in the secondary side is in off state at this time. The transformer T begins to reserve the energy, and the load is supplied by the output capacitor. Then the differential equations of the inductor current and output voltage can be expressed as follows:

$$\frac{di_L}{dt} = \frac{E_{cell} - i_L \cdot R_{on}}{L} \tag{2}$$

$$\frac{dv_c}{dt} = -\frac{v_c}{CR} \tag{3}$$

When the switch is off, the induced voltage of primary side transformer reverses, the diode in the secondary side is in on state at this time. The transformer T begins to release the energy for the load, the magnetic core reset naturally, and the output capacitor is charged. In this state, the differential equations of the inductor current and output voltage can be expressed as follows:

$$\frac{di_L}{dt} = -\frac{v_c + v_D}{nL} \tag{4}$$

$$\frac{dv_c}{dt} = \frac{i_L}{nC} - \frac{v_c}{CR} \tag{5}$$

where R_{on} is the on-resistance of the switch and v_D is the diode voltage drop. According to the KCL and the KVL equilibrium, the state space equation of a non-ideal flyback DC/DC converter can be written as follows:

$$\begin{bmatrix} \frac{di_L}{dt} \\ \frac{dv_c}{dt} \end{bmatrix} = \begin{bmatrix} -\frac{R_{on} \cdot u}{L} & -\frac{1}{nL} \\ \frac{1}{nC} & -\frac{1}{CR} \end{bmatrix} \begin{bmatrix} i_L \\ v_c \end{bmatrix} + \begin{bmatrix} \frac{nE_{cell} + v_c}{nL} \\ -\frac{i_L}{nC} \end{bmatrix} u + \begin{bmatrix} \frac{-v_D}{nL} \\ 0 \end{bmatrix} (1 - u) \tag{6}$$

where n is the transformer turn ratio, u is the control input, v_c is the output voltage, L is the inductance of the primary coil of the transformer T, i_L is the inductor current. C is the capacitor capacitance.

3. High-order sliding mode control

In this section, the high order sliding mode control strategy is developed for the fuel cell power applications. Since the fuel cell output voltage can be influenced under different operating conditions in terms of the varied fuel input (hydrogen) and the air pressure, the controller of the flyback DC/DC converter should satisfy the output voltage and current stabilization requirements of the fuel cell power applications.

SMC is a well-known nonlinear control method for non-linear systems and is renowned for its insensitivity to parametric uncertainty and external disturbance. This technique is based on the discontinuous control law of the system, which can ensure the convergence of the system within a finite time. The output function (sliding variable) can ultimately reach the designed sliding mode manifold. However, SMC suffers from the chattering, finite-amplitude oscillations of the output due to the high-frequency switching of the un-modeled dynamics in the closed loop system. High-order sliding mode (HSM) control is an effective solution to these issues. HSM places the discontinuous term in the high-order derivative of the sliding surface, which can eliminate the chattering of the low-order sliding surface and ultimately achieve the smooth output of the system. Several HSM control algorithms were proposed in Refs. [20,40] for nonlinear systems, including the twisting algorithm, the sub-optimal algorithm, and the super-twisting algorithm. In this paper, the super-twisting algorithm of HSM is applied to achieve the desired stability of the fuel cell power system.

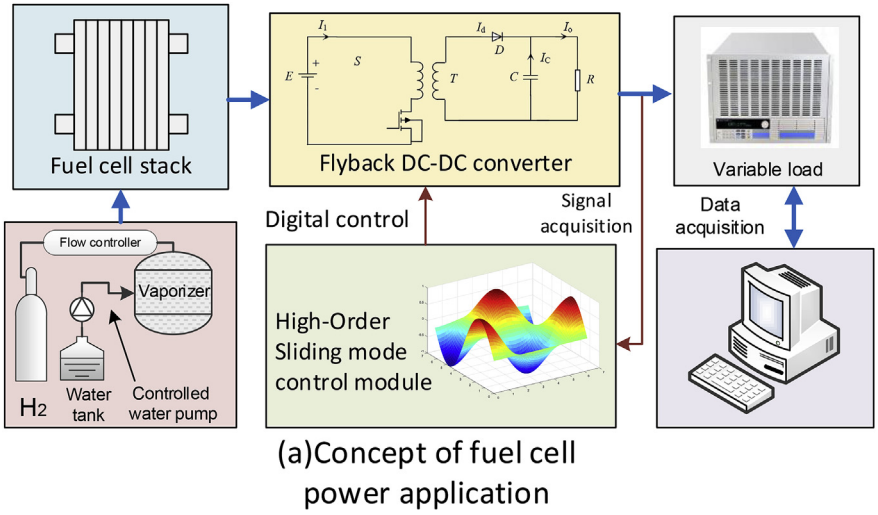

Fig. 1. Fuel cell power application and the flyback DC/DC converter.

3.1. HSM super-twisting control

The super-twisting algorithm has been developed to control systems with relative degree one in order to avoid chattering. The control law in the super-twisting comprises two terms as follows:

$$u(t) = u_1(t) + u_2(t) \tag{7}$$

$$\dot{u}_1 = \begin{cases} -u, & |u| > u_{max} \\ -W\text{sign}(s), & |u| \le u_{max} \end{cases} \tag{8}$$

$$u_2 = \begin{cases} -\lambda |s_0|^{\rho}\text{sign}(s), & |s| > s_0 \\ -\lambda |s|^{\rho}\text{sign}(s), & |s| \le s_0 \end{cases} \tag{9}$$

where W, ρ, λ, and s_0 are all positive constants. The corresponding sufficient conditions for ensuring the finite time convergence to the sliding mode manifold are shown as follows [40]:

$$\begin{cases} W > \frac{\phi}{\Gamma_M} \\ \lambda^2 \ge \frac{4\phi\Gamma_M(W+\phi)}{\Gamma_m^3(W-\phi)} \\ 0 < \rho \le 0.5 \end{cases} \tag{10}$$

where Γ_M, Γ_m, ϕ are positive constants about the bounded conditions. In this paper, the convergence analysis is completed through the Lyapunov stability theorem. The convergence trajectory of the Super-twisting algorithm can converge to the origin (the sliding mode manifold) within a finite time asymptotically.

It is noted that the HSM super-twisting algorithm does not need any differential information of the sliding mode surface, compared with other sliding mode control algorithms. This characteristic of the super-twisting algorithm is very useful for the engineering applications, which means that fewer sensors are needed for the HSM controller, such as the current sensors, etc.

3.2. Digital HSM controller design

For a non-linear system, the state equation can be written as follows:

$$\begin{aligned} \dot{x} &= f(x) + g(x)\cdot u \\ y &= s(x, t) \end{aligned} \tag{11}$$

where x is the system state variable, t is the system time, y is output, u is control input, $f(x)$ is the uncontrolled system function, $g(x)$ is the controlled system function. formula (11) is also a general form of the state space equation (6) of the flyback converter. Specifically, the state variable and output variable is described in (12). For the flyback converter model and the voltage regulator, y is the output voltage, x is a vector composed of the inductor current i_L and capacitor voltage v_c.

$$x = \begin{bmatrix} x_1 \\ x_2 \end{bmatrix} = \begin{bmatrix} i_L \\ v_c \end{bmatrix}, \quad y = x_2 = v_c \tag{12}$$

The sliding mode surface function $s(x)$ of the flyback converter is defined as follows:

$$s(x) = x_2 - x_{2ref} = V_c - V_{ref} \tag{13}$$

where V_c is the output voltage, and V_{ref} is the reference output voltage value of the flyback DC/DC converter. It is clear that the relative degree of the sliding mode surface function is greater than one, and then the HSM control law of the flyback converter can be described as follows:

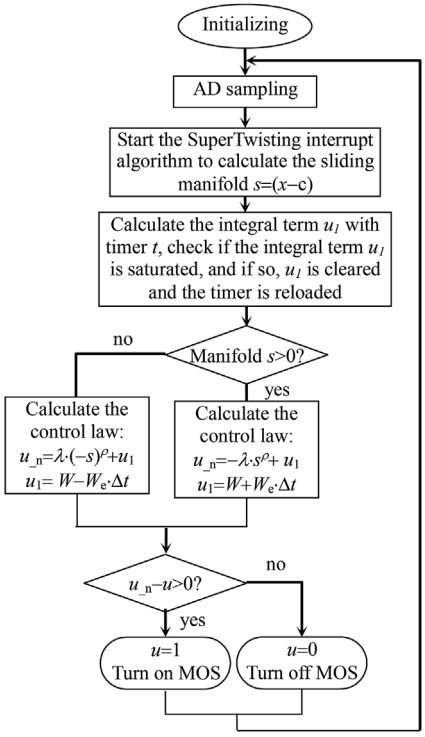

Fig. 2. The program flowchart of the digital HSM controller in DSP.

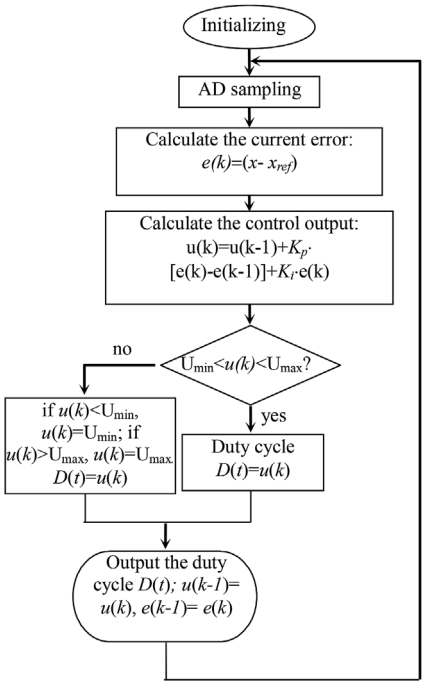

Fig. 3. The program flowchart of the incremental PI control.

$$u = u_1 + u_2 = \int -W\mathrm{sign}(s)\mathrm{d}t - \lambda |s|^{\rho}\mathrm{sign}(s)$$
$$u_1 = -\int W sign(s) dt$$
$$u_2 = -\lambda |s|^{\rho} sign(s) \tag{14}$$

where u is the control signal, which is consisted of two terms, u_1 and u_2. Clearly, u_1 is an integral function, u_2 is an exponential function. Considering different polarities of the sliding mode surface function $s(x)$, the expressions of HSM control law can be rewritten in (15).

$$u = \begin{cases} -\int W\mathrm{d}t - \lambda |s|^{\rho}, & s > 0 \\ \int W\mathrm{d}t + \lambda |s|^{\rho}, & s < 0 \end{cases} \tag{15}$$

Additionally, in order to apply the HSM control in the digital signal processor, the discrete form of the HSM controller is also deduced as follows:

$$u = \begin{cases} -\lambda \cdot s^{\rho} + W \cdot \Delta t + W_0 \ , & s > 0 \\ \lambda \cdot (-s)^{\rho} - W \cdot \Delta t + W_0, & s < 0 \end{cases} \tag{16}$$

According to the discrete form of the HSM controller in (16), the flowchart of the program in the DSP can be designed as shown in Fig. 2. The control law of the digital HSM controller in the experiment (the switching frequency) can reach up to 25 kHz.

Further, the designed digital high-order sliding mode control strategy should converge within a limited time. In order to ensure the theoretical convergence of the proposed digital HSM controller, the Lyapunov stability criteria is adopted to analyze the convergence [41]. Firstly, we can construct a positive definite function as follows:

$$U = \frac{1}{2}s^2 > 0 \tag{17}$$

Then we can obtain the following formula through deriving formula (17) as follows:

$$\dot{U} = s\dot{s} = (x_2 - x_{2ref})(\dot{x}_2 - 0) = (x_2 - x_{2ref})\left(\frac{1}{nC}x_1 - \frac{1}{CR}x_2 - \frac{x_1}{nC}u\right)$$
$$= -\frac{1}{CR}x_2^2 - \frac{x_{2ref}}{CR}x_2 + \frac{x_1}{nC}(x_2 - x_{2ref})(1 - u) \tag{18}$$

According to the output characteristic of the flyback converter, we can know the following conditions can be satisfied.

$$x_{2ref} > 0 \tag{19}$$

$$|x_2 - x_{2ref}| < \delta \tag{20}$$

where δ is a very small positive constant. The control input u is the drive signal of the switch, which satisfies the following conditions:

$$0 \le u \le 1 \tag{21}$$

Thus, substituting formula (19) ~ (21) into (18), it is clear that equation (17) satisfies the following condition:

$$\dot{U} < 0 \tag{22}$$

Hence, according to the Lyapunov stability criteria, it can be concluded that the proposed high-order sliding mode control strategy can converge within a finite time.

3.3. Incremental PI controller

As is well known, the PI (proportional integral) control is a widely used control method in power converters. It is a classical linear control method based on the small signal modelling of power converters. Depending on the dynamic error between the reference and output value, the PI controller can regulate the control signal based on the proportion and the integration of the error signal. The PI control can be described as follows:

$$u = k_p e + k_i \int e\, dt$$
$$e = x - x_{ref} \tag{23}$$

where u is the control signal, e is the error between the reference value and the output, k_p is the proportion coefficient, k_i is the integral coefficient. We can also derive the discrete form of PI control in (24).

$$u(k-1) = K_p e(k-1) + K_i \sum_{j=0}^{k-1} e(j) \tag{24}$$

The traditional PI control suffers from the integral saturation problem which leads to a relatively long settling time in the control process

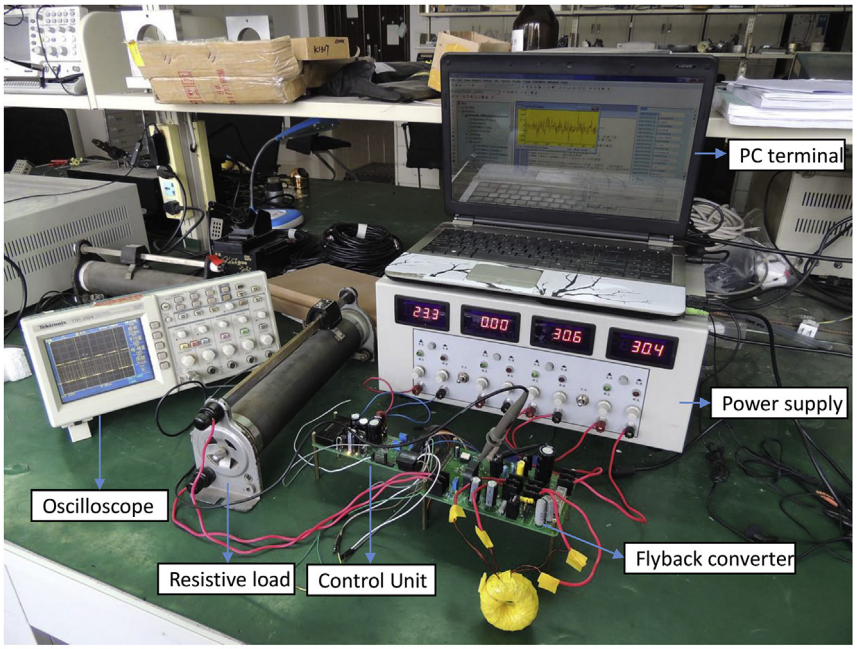

(a)The experimental system

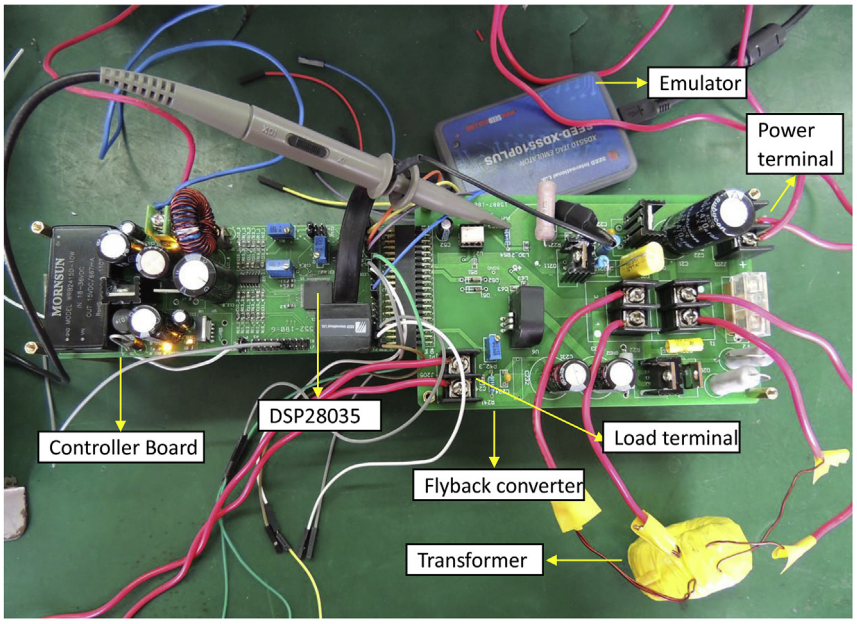

(b) The control unit and the Flyback converter

Fig. 4. The experimental test bench.

[42]. In order to obtain a better dynamic performance, the incremental PI control is adopted in this paper. **According to** formula (24), the expression of the incremental equation PI can be obtained as follows:

$$u(k) = K_p e(k-1) + K_i \sum_{j=0}^{k-1} e(j) + K_p[e(k) - e(k-1)] + K_i e(k) \tag{25}$$

$$u(k) = u(k-1) + K_p[e(k) - e(k-1)] + K_i e(k) \tag{26}$$

Consequently, based on formula (25-26), the program flowchart of the incremental PI control is illustrated in Fig. 3. Every episode of the control process, the control signal is calculated based on the previous control signal, as described in formula (26). Different from the traditional PI control, the computation of the incremental PI controller is reduced a lot, and the saturation issue is also avoided. Hence, the incremental PI controller shows a comprehensive performance, compared with the traditional PI controller.

4. Experiments analysis

In this section, several experiments under different load and input conditions are carried out to verify the effectiveness of the proposed digital high order sliding mode controller for the flyback converter. The control performance is compared with the benchmark scheme, the typical incremental PI controller presented in Section III.

The experimental test bench is shown in Fig. 4. It includes the

Table 2
Experimental parameters.

Elements	Parameters	Value
Power supply	WYK302B4	30 V, 2A, 4 outputs
Oscilloscope	Gwinstek GDS-1102A, Tektronix TDS220	N/A
DSP	TMS320F28035	N/A
DSP Emulator	seed-xds510plus	N/A
Transformer	Turns ratio	2:1
Coil Inductance	Inductance of the primary/secondary coil	2.5 mH/684uH
Snubber RCD circuit	Resistance	3kΩ
	Capacitor	100 nF
	Diode	FR107
MOSFET	SPB17N80	800 V, 17A
Output capacitor	Capacitance	470 μF
Diode	SF56	400 V, 4A
ADC	Sampling rate	60 kHz

control unit, the flyback converter, the DC power supply, the resistive load, and the PC terminal. The digital signal processor (DSP) TMS320F28035 is the control chip in this paper, which has a 32-bit processor and a 12-bit ADC. It supports the float point calculation, and its main frequency can be up to 240 MHZ. The detailed experiment parameters are shown in Table 2.

In order to clearly present the experimental results, the figures are generated from the oscilloscope data using MATLAB. The experiments are divided into two groups: 1) The experiments under load disturbance. 2) The experiments under input voltage disturbance.

4.1. Experiments under load disturbance

4.1.1. Double load disturbance

Firstly, the experiment results obtained under the double load disturbance are shown in Fig. 5(a) and Fig. 5(b), which are controlled by the incremental PI control algorithm and the high order sliding mode control algorithm respectively. The input voltage of the converter is 60 V, and the reference voltage value is 27 V. Meanwhile, in the figures, the blue line is the output voltage, and the red line is the load current. The load variation is realized through a single-pole-double-throw switch. The load current decreases from 0.5A to 0A instantly, and then rises to 1A after about 5 ms.

The control performance of the incremental PI algorithm is shown in Fig. 5(a). The proportion coefficient k_p is 200, the integral coefficient k_i is 1. From Fig. 5(a), it is clear that when the load current changes rapidly, the converter output voltage will show obvious distortions, where the peak value can reach up to 29 V, the settling time is about 17 ms, and the overshoot rate is about 11.1%.

Meanwhile, the control performance under the same experimental condition with the HSM super-twisting algorithm is shown in Fig. 5(b). The control parameters are as follows: $\rho = 0.5$, $\lambda = 2$, $w = 1.2$. It is clear from Fig. 5(b) that, the output voltage can always keep stable when the load current changes intensely, which fully reflects the robustness and the dynamic capacity of the proposed digital high order sliding mode control.

4.1.2. Triple load disturbance

Under the same experimental condition ($k_p = 200$, $k_i = 1$, $\rho = 0.5$, $\lambda = 2$, $w = 1.2$), we conduct the experiments under triple load disturbance. The resistive load involves two sliding rheostats controlled by a single-pole-double-throw switch. The input voltage is 60V, and the reference output voltage value is 27V. Meanwhile, The load current changes from 0.5 A to 0A, and then rises to 1.5A, which lasts for about 8 ms. The control performance of the incremental PI algorithm and the high order sliding mode control are presented in Fig. 6(a) and Fig. 6(b) respectively. From Fig. 6(a), we can observe that the output voltage involves distortions when the load current changes at 0.035s, with a fluctuation amplitude of 3.5 V and an overshoot rate of up to 12.96%. The output voltage achieves convergence after 23 ms. Meanwhile, since the load current increases significantly, the steady-state error and the output ripple waves also increase, the steady-state error rate is about 3.3%.

On the other hand, it is clear that the output voltage can always remain stable with the digital high-order mode control, as is shown in Fig. 6(b). The load current changes from 0.5A to 0A at 0.035s, before it rapidly changes from 0A to1.5A at 0.04s. Though the load current variation is drastic and the variation range is sufficiently wide (0.5A-0A-1.5A), the system could still achieve a fast convergence under the digital HSM control. During the three stages of load disturbance (0.5A-0A-1.5A within 10 ms), the settling time of the flyback power converter is less than 0.1 ms, while the overshoot is small enough to be neglected.

4.1.3. Quadruple load disturbance

In order to further test the performance of the digital HSM controller designed for the flyback power converter, the experiments of 4 times load disturbance are conducted, and the results are shown in Fig. 7(a) and Fig. 7(b). The load current changes from 0.5A to 0A, and rises to 2.1A instantly, which lasts for about 10 ms.

The control performance of the incremental PI control is shown in Fig. 7 (a). We can observe that the output voltage takes distortion when the load current changes at 0.022s, with a fluctuation amplitude of 3.8 V and an overshoot rate of up to 14.07%. The output voltage achieves convergence after 31 ms. During the 3 stages of load disturbance (0.5A-0A-2.1A), the output steady-state error and ripple waves also have some increase after the convergence, due to the

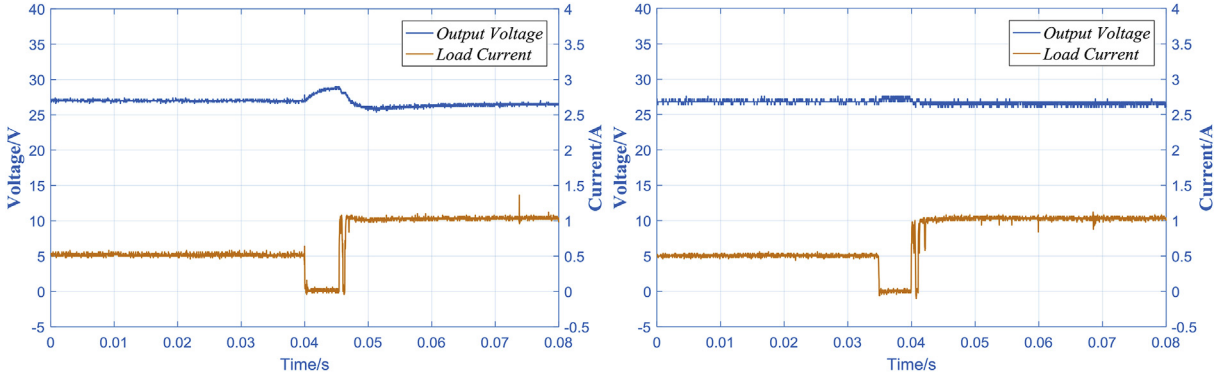

(a) PI control under twice the load disturbance

(b) HSM control under twice the load disturbance

Fig. 5. Experiments under twice the load disturbance.

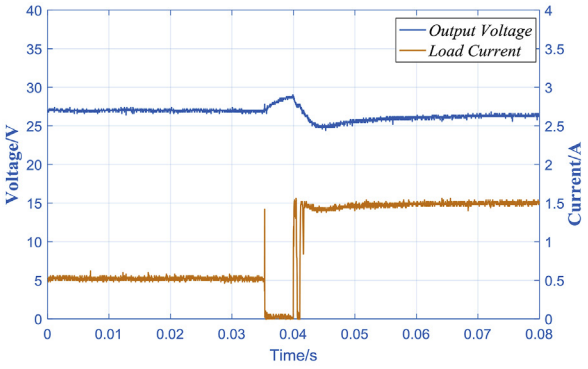

(a) PI control under 3 times the load disturbance

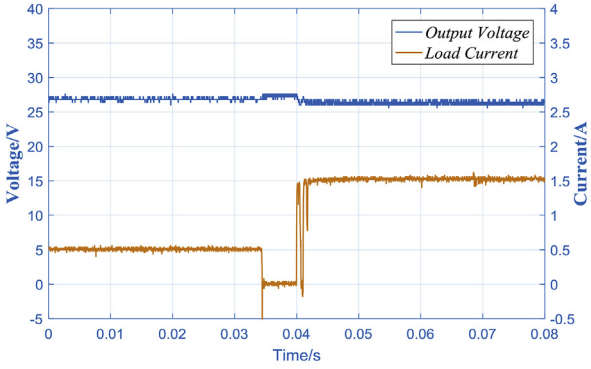

(b) HSM control under 3 times the load disturbance

Fig. 6. Experiments under 3 times the load disturbance.

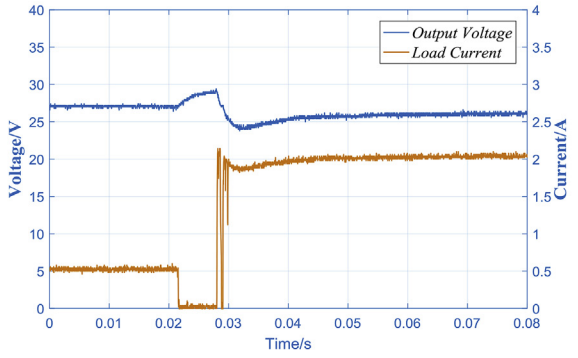

(a) PI control under 4 times the load disturbance

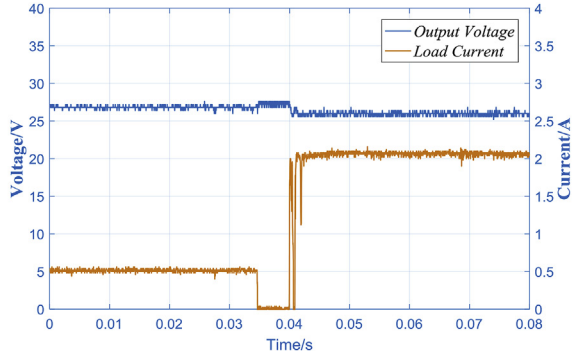

(b) HSM control under 4 times the load disturbance

Fig. 7. Experiments under 4 times the load disturbance.

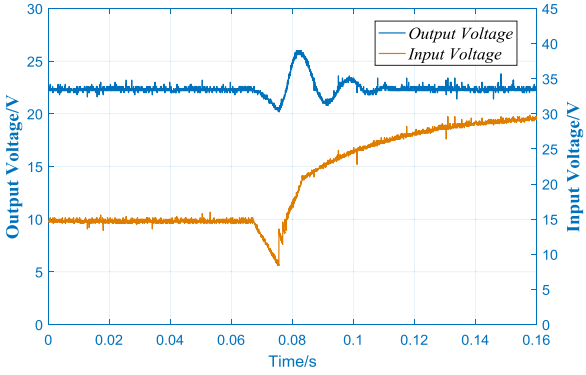

(a) PI control under input voltage disturbance

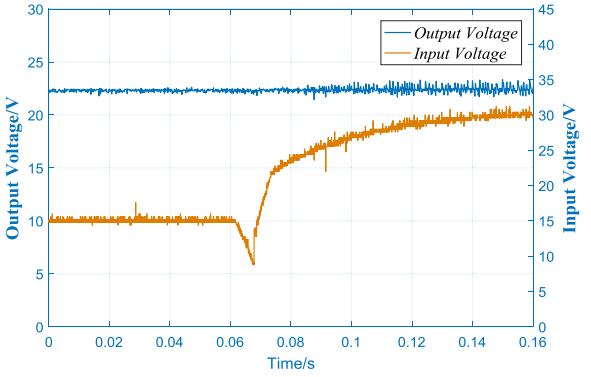

(b) HSM control under input voltage disturbance

Fig. 8. Experiments under input voltage disturbance.

significant increasing load.

Under the same conditions, the digital HSM control performance is shown in Fig. 7 (b). The output voltage can remain stable without fluctuations under the drastic load disturbance, except for a minor steady-state error caused by the significant increasing load current. It is noted that under a drastic load variation condition (0.5A-0A-2.1A within 10 ms), the flyback converter could achieve a fast convergence without voltage overshoots. Thus, through the load disturbance experiments in this section, the robustness and dynamic capacity of the digital HSM controller are fully demonstrated.

4.2. Experiments under input voltage disturbance

In the previous section, the experiments under different load disturbances are conducted to verify the effectiveness of the proposed HSM control method, which could provide a highly robust performance without chattering or voltage overshoot.

In this section, the focus is on the experiments conducted under input voltage disturbances. In order to earn the maximum power in the fuel cell generation applications, the output voltage of fuel cells varies with the output power. Here, the input disturbance experiments can simulate the output voltage variations of fuel cell generations. The experiment results are shown in Fig. 8 (a) and Fig. 8 (b). The reference

Table 3
Comparisons between HSM control and PI control.

Control Algorithm	Disturbance condition	Overshoot rate/%	Settling time/ms	Steady error/%
Incremental PI	0.5—0—1A	11.11	17	2.2
	0.5—0—1.5A	12.96	23	3.3
	0.5—0—2.1A	14.07	31	3.7
	15 V−30 V	26.01	35	0
High-order sliding mode	0.5—0—1A	< 0.1	< 0.1	1.1
	0.5—0—1.5A	< 0.1	< 0.1	2.2
	0.5—0—2.1A	< 0.1	< 0.1	2.9
	15 V−30 V	< 0.1	< 0.1	0

voltage is set at 22.5 V, while the input voltage changes from 15 V to 30 V, as is represented by the red lines in the figures.

The incremental PI control performance is shown in Fig. 8(a). From Fig. 8(a), it is clear that the output voltage distorts when the input voltage changes. The fluctuation amplitude is up to 5.8 V, while the overshoot rate is approximately 26.01%, and the convergence time is 29 ms. After a short period of voltage fluctuations, the output voltage is restored to the reference signal under the incremental PI control.

On the other hand, the HSM control performance under the same experimental conditions is shown in Fig. 8(b). We can observe that the output voltage can keep stable when the input voltage changes. The experimental results thus explicitly demonstrate the robustness and stability of the proposed digital HSM control method.

4.3. Experiment results analysis

Based on the conducted experiments, the corresponding data are summarized in Table 3, including the experimental conditions, the output voltage overshoot rate, the settling time under disturbance, and the steady-state error. From the comparison results in Table 3, the advantages of the proposed HSM controller are clearly illustrated.

The digital HSM controller can achieve a stronger robustness and an improved dynamic performance under large input voltage variation and load disturbance: 1) Under different conditions of load disturbance, the instantaneous output voltage overshoot rate of the flyback converter can reach up to 14% with the incremental PI controller, while the output overshoot rate is less than 0.1% with the digital HSM controller. 2) Under the condition of double input voltage disturbance, the instantaneous output overshoot of the flyback power converter can reach over 25% with the incremental PI controller, while the output overshoot rate is less than 0.1% with the digital HSM controller.

With regard to the dynamic performance in the experiments, the incremental PI control takes about 17–35 ms to converge under different load or input voltage disturbance conditions. Moreover, we can conclude that the larger load disturbance will lead to a corresponding longer settling time. Yet the digital HSM controller of the flyback converter takes less than 0.1 ms to converge under different load or input voltage disturbance conditions.

Thus, compared with the typical incremental PI control, the digital HSM control shows a superior performance in terms of stability, robustness, dynamic capacity, and convergence.

4.4. Discussions

The performance summary and comparisons with some other reported experimental studies are listed in Table 4 Different from the experimental studies in Refs. [22,24,28], and [33], experiments with both input voltage and load disturbance are conducted here, and the disturbance conditions appear to be more drastic in this study. We can also know from Table 4 that the proposed digital HSM controller for the flyback DC/DC converter performs better in terms of the settling time and voltage overshoot, which are important system parameters in power applications.

As well known, the flyback converter has a zero point in the right-half plane of its transfer function. This zero point seriously affects the dynamic performance and cannot be eliminated through a feedback control, meaning it can lead to obvious output distortions. The experiment results in this study demonstrate that the proposed digital HSM controller can effectively improve the robustness, dynamic capacity, and the stability of the flyback converter, which is significant for many power applications with large perturbations. Hence, for the fuel cell power applications [35,36,43,44], the proposed strong robust flyback power converter can be used to harvest the maximum generation power or to regulate the output voltage to feed the subsequent electrical devices.

Moreover, in addition to the fuel cell power applications we focus on in this paper, we also note that it would be valuable to apply the digital HSM controller within a hybrid energy system incorporating PV generation or wind turbine generation. With the higher penetration of renewable energy in the power systems, robust control strategies are required to deal with the intermittency and randomness that exist in the power generation process. Thus, the digital HSM control proposed in this study could provide an effective option to improve the robustness and stability of a hybrid energy system. Given the increasing interests in utilizing PV generation and wind generation to decrease the greenhouse gases involved in power industries [45,46], it would prove valuable to combine the HSM controller with the MPPT technique in a hybrid energy system. This will not only enable the maximum power harvesting of renewable energy, but will also improve the DC-link voltage stability. However, while the proposed digital HSM controller operates well in the flyback DC/DC converter that could be useful in PV generation applications, the power level of the converters still requires certain upgrading for the wind generation applications.

With regards to our future work, it would be interesting to develop the digital HSM controller such that it can be applied in an AC/DC power converter. This could provide fast voltage and frequency support in a grid-connected hybrid energy micro-grid. Furthermore, improving the digital HSM controller to be applied in other high power DC-DC power converters could be another valuable task, which could extend its applications to a wider range.

5. Conclusions

Aiming to solve the problem of load and output disturbance characteristics in fuel cell power applications, an all-digital high-order sliding mode (HSM) controller is designed for the flyback DC/DC converter in this paper. A common digital signal processor TMS320F28035

Table 4
Performance summary and comparisons.

Literature	Power Converter (power level)	Control Algorithm	Settling Time under Disturbance	Over-shoot Rate
2013, L. Martinez-Salamero et al. [22],	Boost (50 W)	SMC	2.5 ms (20 W–40 W)	10%
2015, A. Dashtestani et al. [28],	Buck (1 W)	SMC	5 μs (0–0.72 W)	5%
2017, S. M. Rakhtala et al. [33],	Buck (20 W)	HSM (Twisting)	8 ms (2.5 W–12.5 W)	10%
2017, S. H. Chincholkar et al. [24],	Cascade Boost (5 W)	SMC	~100 ms (1.21 W–2.42 W)	~10%[a]
This work	Flyback (80 W)	HSM(Super-twisting)	< 0.1 ms (load: 13.5 W–0 W to 56.7 W or input: 15 V–30 V)	< 0.1%

[a] Not reported, extracted from the plots.

is used to realize the digital HSM control method. The effectiveness of the proposed digital HSM control method for the flyback converter is verified through several different experiments, while a typical incremental PI control is designed as the benchmark method. Compared with the classical PI control, the proposed digital HSM control can achieve a stronger robustness and a better dynamic performance under different load and input voltage disturbance conditions.

Acknowledgements

Sincere thanks to the financial support of China Scholarship Council (CSC). This work was also partly supported by the National Natural Science Foundation of China under Grant No.61873343, and the Key Cultivation Program of Transformation for Scientific and technological achievements of Xi'an under Grant No.2017KE0100.

References

[1] F. Manzano-Agugliaro, A. Alcayde, F.G. Montoya, A. Zapata-Sierra, C. Gil, Scientific production of renewable energies worldwide: an overview, Renew. Sustain. Energy Rev. 18 (February) (2013) 134–143.
[2] W.Q. Tao, C.H. Min, X.L. Liu, Y.L. He, B.H. Yin, W. Jiang, Parameter sensitivity examination and discussion of PEM fuel cell simulation model validation. Part I. Current status of modeling research and model development, J. Power Sources 160 (1) (2006) 359–373.
[3] M.A.R.S. Al-Baghdadi, Modelling of proton exchange membrane fuel cell performance based on semi-empirical equations, Renew. Energy 30 (10) (2005) 1587–1599.
[4] M.Y. El-Sharkh, A. Rahman, M.S. Alam, P.C. Byrne, A.A. Sakla, T. Thomas, A dynamic model for a stand-alone PEM fuel cell power plant for residential applications, J. Power Sources 138 (1–2) (2004) 199–204.
[5] R.D. Middlebrook, S. Cuk, A general unified approach to modeling switching-converters, Int. J. Eletronics 42 (1977) 521–550 June.
[6] A. Emadi, A. Khaligh, C.H. Rivetta, G.A. Williamson, Constant power loads and negative impedance instability in automotive systems: definition, modeling, stability, and control of power electronic converters and motor drives, IEEE Trans. Veh. Technol. 55 (4) (2006) 1112–1125.
[7] M. Hatti, M. Tioursi, Dynamic neural network controller model of PEM fuel cell system, Int. J. Hydrogen Energy 34 (11) (2009) 5015–5021.
[8] M.Y. El-Sharkh, A. Rahman, M.S. Alam, Neural networks-based control of active and reactive power of a stand-alone PEM fuel cell power plant, J. Power Sources 135 (1–2) (2004) 88–94.
[9] V. Tejwani, B. Suthar, Power management in fuel cell based hybrid systems, Int. J. Hydrogen Energy 42 (22) (2017) 14980–14989.
[10] R. Saadi, et al., Dual loop controllers using PI, sliding mode and flatness controls applied to low voltage converters for fuel cell applications, Int. J. Hydrogen Energy 41 (42) (2016) 19154–19163.
[11] K. Tanaka, T. Ikeda, H.O. Wang, Robust stabilization of a class of uncertain nonlinear systems via fuzzy control: {Quadratic} stabilizability, {H-infinity} control theory, and linear matrix inequalities - Reply, IEEE Trans. Fuzzy Syst. 5 (4) (1997) 630.
[12] J.H. Park, G.T. Park, S.H. Kim, C.J. Moon, Output-feedback control of uncertain nonlinear systems using a self-structuring adaptive fuzzy observer, Fuzzy Set Syst. 151 (1) (2005) 21–42.
[13] D. Wang, J. Huang, Neural network-based adaptive dynamic surface control for a class of uncertain nonlinear systems in strict-feedback form, IEEE Trans. Neural Network. 16 (1) (2005) 195–202.
[14] J. Yu, B. Chen, H. Yu, C. Lin, L. Zhao, Neural networks-based command filtering control of nonlinear systems with uncertain disturbance, Inf. Sci. 426 (2018) 50–60.
[15] S. Zheng, W. Li, Adaptive control for switched nonlinear systems with coupled input nonlinearities and state constraints, Inf. Sci. 462 (2018) 331–356.
[16] J. Zhou, C. Wen, W. Wang, Adaptive control of uncertain nonlinear systems with quantized input signal, Automatica 95 (2018) 152–162.
[17] H. Guldemir, Sliding mode control of Dc-Dc converters, J. Appl. Sci. 5 (3) (2005).
[18] S.C. Tan, Y.M. Lai, C.K. Tse, General design issues of sliding-mode controllers in DC-DC converters, IEEE Trans. Ind. Electron. 55 (3) (2008) 1160–1174.
[19] V. Utkin, Sliding mode control of DC/DC converters, J. Franklin Inst. 350 (8) (2013) 2146–2165.
[20] A. Levant, Higher-order sliding modes, differentiation and output feedback control, Int. J. Contr. 76 (9/10) (2003) 924–941.
[21] A. Levant, Principles of 2-sliding mode design, Automatica 43 (4) (2007) 576–586.
[22] L. Martinez-Salamero, G. Garcia, M. Orellana, C. Lahore, B. Estibals, Start-up control and voltage regulation in a boost converter under sliding-mode operation, IEEE Trans. Ind. Electron. 60 (10) (2013) 4637–4649.
[23] O. Lopez-Santos, L. Martinez-Salamero, G. Garcia, H. Valderrama-Blavi, T. Sierra-Polanco, Robust sliding-mode control design for a voltage regulated quadratic boost converter, IEEE Trans. Power Electron. 30 (4) (2015) 2313–2327.
[24] S.H. Chincholkar, W. Jiang, C.-Y. Chan, An improved PWM-based sliding-mode controller for a dc-dc cascade boost converter, IEEE Trans. Circuits Syst. II Express Briefs (1–1) (2017).
[25] A.G. Perry, G. Feng, Y.F. Liu, P.C. Sen, "A new sliding mode like control method for buck converter," *PESC Rec*, IEEE Annu. Power Electron. Spec. Conf. 5 (2004) 3688–3693.
[26] J. Kim, M.A. Horowitz, An efficient digital sliding controller for adaptive power-supply regulation, IEEE J. Solid State Circ. 37 (5) (2002) 639–647.
[27] F. Luo, S. Member, D. Ma, S. Member, "Design of digital tri-mode adaptive-output buck – boost power converter for power-efficient integrated systems, 57 (6) (2010) 2151–2160.
[28] A. Dashtestani, B. Bakkaloglu, A fast settling oversampled digital sliding-mode DC-DC converter, IEEE Trans. Power Electron. 30 (2) (2015) 1019–1027.
[29] M. Farhat, O. Barambones, L. Sbita, A new maximum power point method based on a sliding mode approach for solar energy harvesting, Appl. Energy 185 (2017) 1185–1198.
[30] M. Farhat, O. Barambones, L. Sbita, Real-time efficiency boosting for PV systems using MPPT based on sliding mode, Energy Procedia 75 (2015) 361–366.
[31] M. Derbeli, M. Farhat, O. Barambones, L. Sbita, Control of PEM fuel cell power system using sliding mode and super-twisting algorithms, Int. J. Hydrogen Energy 42 (13) (2017) 8833–8844.
[32] N. Chatrenour, H. Razmi, H. Doagou-Mojarrad, Improved double integral sliding mode MPPT controller based parameter estimation for a stand-alone photovoltaic system, Energy Convers. Manag. 139 (2017) 97–109.
[33] S.M. Rakhtala, M. Yasoubi, H. HosseinNia, Design of second order sliding mode and sliding mode algorithms: a practical insight to DC-DC buck converter, IEEE/CAA J. Autom. Sin. 4 (3) (2017) 483–497.
[34] B. Wang, G. Ma, D. Xu, L. Zhang, J. Zhou, Switching sliding-mode control strategy based on multi-type restrictive condition for voltage control of buck converter in auxiliary energy source, Appl. Energy 228 (June) (2018) 1373–1384.
[35] J.T. Babauta, M. Kerber, L. Hsu, A. Phipps, D.B. Chadwick, Y.M. Arias-Thode, Scaling up benthic microbial fuel cells using flyback converters, J. Power Sources 395 (2018) 98–105.
[36] M. Alaraj, Z.J. Ren, J. Do Park, Microbial fuel cell energy harvesting using synchronous flyback converter, J. Power Sources 247 (2014) 636–642.
[37] R.W. Erickson, D. Maksimovic, Fundamentals of Power Electronics, Springer-Verlag, New York, NY, USA, 2007.
[38] H. Hu, V. Yousefzadeh, D. Maksimović, Nonuniform A/D quantization for improved dynamic responses of digitally controlled DC-DC converters, IEEE Trans. Power Electron. 23 (4) (2008) 1998–2005.
[39] Rui MA, Yu Wu, Elena Breaz, yigeng Huangfu, Pascal Briois, Fei Gao, High-order sliding mode control of DC-DC converter for PEM fuel cell applications, Proc. IEEE IAS Annu. Meeting, Oct. 2018.
[40] A. Levant, L. Fridman, Higher-order Sliding Modes, (2002).
[41] H.K. Khalil, "Non linear systems," prentice-Hall, New Jersey 2 (5) (1996) 1–5.
[42] K.J. Åström, T. Hägglund, The future of PID control, Contr. Eng. Pract. 9 (11) (2001) 1163–1175.
[43] M. Alaraj, M. Radenkovic, J. Do Park, Intelligent energy harvesting scheme for microbial fuel cells: maximum power point tracking and voltage overshoot avoidance, J. Power Sources 342 (2017) 726–732.
[44] N. Benyahia, H. Denoun, A. Badji, M. Zaouia, T. Rekioua, N. Benamrouche, D. Rekioua, MPPT controller for an interleaved boost dc-dc converter used in fuel cell electric vehicles, Int. J. Hydrogen Energy 39 (27) (2014) 15196–15205.
[45] S. Tamalouzt, N. Benyahia, T. Rekioua, D. Rekioua, R. Abdessemed, Performances analysis of WT-DFIG with PV and fuel cell hybrid power sources system associated with hydrogen storage hybrid energy system, Int. J. Hydrogen Energy 41 (45) (2016) 21006–21021.
[46] Y. Bouzelata, N. Altin, R. Chenni, E. Kurt, Exploration of optimal design and performance of a hybrid wind-solar energy system, Int. J. Hydrogen Energy 41 (29) (2016) 12497–12511.